

ARLIS Interlibrary Loan



ILLiad TN: 40273

Borrower: GIE

Lending String: *RLA,ISU

Patron: G. Chander

Journal Title: Canadian journal of remote sensing.

Volume: 23 **Issue:**
Month/Year: 1997**Pages:** 309?317

Article Author:

Article Title: Reflectance- and Irradiance-Based
Calibration of Landsat-5 Thematic Mapper/Thome,
K. J.

Imprint: Ottawa ; Canadian Aeronautics and
Space

ILL Number: 33223022



Call #:

Location:

**Mail
Charge
Maxcost:** 20.00IFM

Shipping Address:
USGS-EROS
ATTN: Library - ILL
Mundt Federal Building
Sioux Falls, SD 57198-0001

Fax: 605-594-2725
Ariel: cdeering@usgs.gov



Thank you for using ARLIS Interlibrary Loan

We want to provide you with the best copy possible. Please let us know of any problems by contacting us within five working days. ARLIS ILL staff can be reached at:

Cory, Interlibrary Loan Lending
907-786-7679
cory@arlis.org

Sharon, Interlibrary Loan Borrowing
907-786-7677
sharon@arlis.org

Fax 907-786-7680
ill@arlis.org

Copyright Warning

The copyright law of the United States (Title 17, United States Code) governs the making of photocopies or other reproductions of copyrighted material.

Under certain conditions specified in the law, libraries and archives are authorized to furnish a photocopy or other reproduction. One of these specified conditions is that the photocopy or reproduction is not to be "used for any purpose other than private study, scholarship, or research." If a user makes a request for, or later uses, a photocopy or reproduction for purposes in excess of "fair use," that user may be liable for copyright infringement.

This institution reserves the right to refuse to accept a copying order, if in its judgment, fulfillment of the order would involve violation of copyright law.

Reflectance- and Irradiance-based Calibration of Landsat-5 Thematic Mapper

Research Note/Note de recherche

by K.J. Thome • B.G. Crowther • S.F. Biggar

RÉSUMÉ

On utilise des méthodes basées sur la réflectance et l'éclairement pour effectuer l'étalonnage radiométrique absolu du capteur Thematic Mapper de Landsat-5 dans la partie réfléchie du rayonnement solaire du spectre pour des données utilisant le format du Landsat Archive Production System. Les résultats présentés proviennent d'une campagne d'étalonnage réalisée en décembre 1996 à la base de White Sands Missile Range, Nouveau-Mexique. Les résultats des deux méthodes concordent dans une proportion meilleure que 6% et des comparaisons avec des luminances prédites au niveau du capteur à partir des gains et des biais fournis avec les images ont permis de déceler des variations de 1% à 31%. On compare également ces résultats avec ceux dérivés précédemment à l'aide de différentes techniques de traitement. Les différences considérables observées entre ces résultats et les valeurs réelles démontrent l'importance de l'utilisation judicieuse de procédures d'étalonnage des données de télédétection.

SUMMARY

The reflectance- and irradiance-based methods are used to determine an absolute, radiometric calibration of Landsat-5 Thematic Mapper for the solar reflective portion of the spectrum for data using the National Landsat Archive Production System format. Results are given for a calibration campaign at White Sands Missile Range in New Mexico in December 1996. The results of the two methods agree to better than 6% and comparisons with predicted, at-sensor radiances based on the gains and biases supplied with the data tape were found to differ by 1% to 41%. The results are also presented with reference to previously determined results from different processing techniques. The large differences between these results and the current values indicate the importance of consistent use of calibration for remotely-sensed data.

INTRODUCTION

As remote sensing has become more quantitative over time, sensor calibration has become an important issue for quantitative temporal studies of surface features. Without accurate sensor calibration, temporal changes could be masked by sensor degradation and in-flight, absolute calibration of satellite sensors is needed to determine the magnitude of degradation. These in-flight methods have relied on both onboard systems and vicarious methods. Here the term "vicarious" refers to in-flight methods that do not use onboard systems. Typical onboard systems include direct solar illumination, solar diffusers, and onboard lamps. These systems provide calibration at high temporal frequency to determine instrument response trends. As an example, onboard lamps have been used successfully for Système Pour l'Observation de la Terre Haute Résolution Visible (SPOT HRV) (Gellman *et al.*, 1993). The problem with onboard calibration systems is that they can degrade over time, or may themselves have biases which affect the calibration. Vicarious methods have an advantage in that they provide an independent means of absolute calibration using a full-system, full-aperture calibration. These vicarious methods also calibrate the sensor in a mode in which it is normally operated.

The Remote Sensing Group (RSG) of the Optical Sciences Center at the University of Arizona has been using vicarious methods since the early 1980s (Slater *et al.*, 1987). Early calibrations were of Landsat Thematic Mapper (TM) (Slater *et al.*, 1987), but later work has included the SPOT HRV sensors (Gellman *et al.*, 1993 and Biggar *et al.*, 1991), and several airborne sensors (Balick *et al.*, 1991, and Thome *et al.*, 1996). The RSG has developed three techniques of absolute calibration that rely on measurements at a well-characterized ground target at the same time as a satellite overpass.

In the radiance-based method, a well-calibrated radiometer is flown over a target at the same time the satellite sensor views the target (Slater *et al.*, 1987). This approach is the most accurate of the three used by the RSG, with uncertainties as low as 3%

• K.J. Thome, B.G. Crowther, S.F. Biggar are with the Remote Sensing Group, Optical Sciences Center, University of Arizona, P.O. Box 210094, Tucson, Arizona 85721-0094

(Biggar *et al.*, 1994). The primary advantage to such an approach is that the radiometer can be flown over much of the scattering influences of the atmosphere, thus minimizing uncertainties in radiance estimates due to atmospheric variation. While accurate, the cost and difficulties involved in flying these radiometers can be problematic. Thus, the radiance-based approach has not been used as often as the other two methods, referred to as the reflectance- and irradiance-based approaches.

The reflectance-based method relies on ground-based measurements of both the surface reflectance and the atmospheric extinction at the time of satellite overpass. These measurements are used to find required inputs for a radiative transfer code to predict top-of-the-atmosphere radiances. Comparisons between the reported digital numbers (DNs) of the site with these predicted radiances give the calibration of the system. The irradiance-based approach is similar, but uses measurements of the downwelling solar and sky irradiances to further constrain the results from the radiative transfer codes (Biggar *et al.*, 1990b). In the past, these diffuse irradiance measurements were made by blocking a reflectance panel with a large parasol. Because of the labor-intensive nature of these diffuse irradiance measurements, the method has not seen widespread use.

In the current work, we compare results from both methods using data from a recent campaign to White Sands Missile Range to calibrate the Landsat-5 TM. This is the first attempt at calibrating TM using an irradiance-based approach and to do so we made use of a recently-developed instrument for measuring the downwelling irradiances needed for the method (Crowther, 1997). TM provides an interesting test of the irradiance-based approach because of the short-wavelength band in the blue portion of the spectrum. There is a larger amount of diffuse light in this portion of the spectrum, and, as will be discussed later, this increases the uncertainties of the reflectance-based results relative to the irradiance-based results.

We begin by giving a more detailed description of the reflectance- and irradiance-based methods, including descriptions of the calibration site, measurements of surface reflectance and atmospheric properties, determination of average image digital numbers (DN) for the site, and radiative transfer code. The newly-developed, diffuse-to-global instrument is briefly described followed by an error discussion. Finally, the results from the data collected at White Sands Missile Range on December 16, 1996 are presented for TM image data processed using the National Landsat Archive Production System (NLAPS).

METHOD

Reflectance-based approach

The reflectance-based approach relies on ground-based surface reflectance measurements of a selected target at the time of sensor overpass. The atmosphere over the target is characterized using measurements from solar radiometers to determine columnar amounts of absorbing gases and the scattering properties of the aerosols. The results of the surface and atmospheric characterization are used as input to a radiative transfer code to predict the top-of-the-atmosphere radiance. The digital

numbers reported by the sensor are compared to these predicted radiances to give a radiometric calibration. Each portion of this technique is now described in more detail.

Test Site

The site used for this work is part of the alkali-flats area of White Sands Missile Range, New Mexico and is referred to as Chuck Site. The characteristics of this area, used by the RSG since the early 1980s, are well-understood. The target used for the TM work is a 120-m × 480-m rectangular area oriented approximately in the ground-track direction of the satellite to give 4 columns and 16 rows for the solar-reflective bands of TM. The number of rows ensures that data from the target are collected for each of the 16 detectors of each spectral band in the solar-reflective part of the spectrum.

Surface Reflectance

Accurate determination of the surface reflectance of the test site is critical for both the reflectance- and irradiance-based methods. We find the surface reflectance of the site by ratioing radiometer measurements of the site to those from a panel made from an aluminum sheet painted with barium sulfate. The reflectance of this panel is assumed to be known from calibrations made in the facilities of the RSG (Biggar *et al.*, 1988). These BR/ measurements are used in a software package developed by the RSG that accounts for effects due to sun-angle changes during the measurement period. The method is to measure the upwelling radiance from the reference panel at several points in time during the data collection. These measurements are correlated with the BR/ computed for the incident solar angle based on the laboratory measurements. The reflectance is determined by ratioing a measurement of the test site to a predicted signal expected from the reference panel at the time of the site measurement. While we also collect global irradiance data to measure changes in diffuse skylight illumination, these data are not used to correct the predicted panel signals, but rather they are used to evaluate the quality of the overall data set. This is not a problem for the data sets presented here because the atmospheric turbidity is low at the White Sands site. In addition, the panel and surface reflectances are both high, thus the dominant effect is due to changes in the incident solar energy. For all of the data sets, this variability is small compared to the uncertainties of the measurements.

Past field measurements were made by carrying an eight channel, Barnes Modular Multispectral Radiometer (MMR)¹ across the entire site. The MMR nominally duplicates the six TM solar-reflective bands (Robinson *et al.*, 1979) and is used with a 15 degree, full-width at half-maximum (FWHM) field of view. The instrument is usually attached to a backpack device or yoke that is carried across the site but has, on two occasions, been attached to a space frame connected to a trailer that was towed across the site. In the case of the yoke, the user collects

¹Trade names and company names are included for the convenience of the reader and imply no endorsement of the product or company by the University of Arizona.

10 reflectance samples along a straight-line path within each of the 64, 30-m \times 30-m areas of the site representing 64 TM pixels. A total of 640 points are collected over the entire 120-m \times 480-m area. Reflectance of the test site is determined by averaging all 640 measurements to provide one set of spectral reflectances that are compared to the average DNs of the site determined from the Landsat imagery.

The trailer approach was essentially identical, although about half as many points were collected because it took less time for the trailer to cover the site. The advantage to the "reflectomobile" was that it gave us the flexibility to measure reflectance with several instruments at one time and to use much heavier instruments. Unfortunately, the surface of our test site is soft enough that the tow vehicle and reflectomobile trailer left tire tracks that covered about 4% of the total area of the site. The effect of these tracks on the retrieved site reflectance of the TM site was <1.0%, but since the effect is larger for smaller footprint sensors, we have returned to walking radiometers across our site to prevent scarring the site for future work.

More recently, we have begun making measurements of the site reflectance using an Analytic Spectral Devices FieldSpec Full Range (ASD FR) spectrometer. This system collects data over the spectral range from 350 to 2500 nm at 1.4-nm intervals in the 350- to 1000-nm range and 10-nm intervals in the 1000- to 2500-nm range. The nominal channel bandpasses are on the order of 10 nm. This instrument is used with an eight-degree, FWHM field of view in an identical fashion as the MMR and we collect 10 points per "pixel" with each point being an average of 30 spectra. An average of 640 points from the ASD FR collected on September 5, 1996 of our SPOT-HRV test site are shown in **Figure 1**. Also on this graph are spectral transmittances of the filters used in the MMR as measured by a monochromator in the laboratory. Comparisons of the average reflectance of 640 MMR data points and the ASD FR results are shown in **Table 1**. The reflectance results for the ASD FR have been band-averaged using the filter transmittance data shown in **Figure 1**. The standard deviations of

Table 1.

September 5, 1996 surface reflectance results from White Sands for both the MMR and ASD FR instruments. The ASD FR results have been band averaged using the MMR filter transmittances. Also shown are the 1- σ standard deviations of the average of the MMR results.

MMR wavelength (nm)	MMR	1- σ std. dev.	ASD FR
491	0.486	6.2%	0.495
562	0.548	5.8%	0.558
663	0.590	5.6%	0.602
812	0.625	5.6%	0.639
1254	0.608	6.1%	0.629
1688	0.489	7.6%	0.481
2217	0.226	9.4%	0.220

the average of the MMR data are also shown in the table. From the table, it can be seen that the agreement between the two instruments is quite good, especially when one considers the standard deviation of the MMR reflectance data and the fact that the instruments do not measure identical portions of the site. In all cases, the percent difference between the band-averaged ASD FR data and MMR data is less than the uncertainty caused by the site inhomogeneity, as implied by the standard deviations of the average of the reflectances, indicating that the use of the ASD FR should not bias the results. These results also indicate that the precision of the surface reflectance measurements for the TM site at White Sands is about 2%, but that there is poorer agreement in the shortwave infrared. This is most likely due to a temperature effect in the MMR because the instrument is not thermally stabilized and is known to be temperature sensitive in the shortwave infrared.

Atmospheric Scattering and Absorption

The primary instrument used to characterize the atmosphere over Chuck Site is the solar radiometer. In this work we use a ten-band system in a Langley method retrieval scheme to determine spectral-atmospheric optical depths (Gellman *et al.*, 1991). The optical depth results are used as part of an inversion scheme developed by the RSG to determine ozone optical depth and a Junge aerosol size distribution parameter (Biggar *et al.*, 1990a). The Junge parameter, in turn, is used to determine the optical depths at the wavelengths of the six solar-reflective bands of TM using Angstrom's turbidity law. Three near-infrared bands of the radiometer are part of a columnar water vapor retrieval using a modified Langley approach (Thome *et al.*, 1992). The retrieved columnar water vapor is used in the 6S radiative transfer code to determine band-integrated transmittances for the TM wavelengths for the sun-to-surface-to-satellite path.

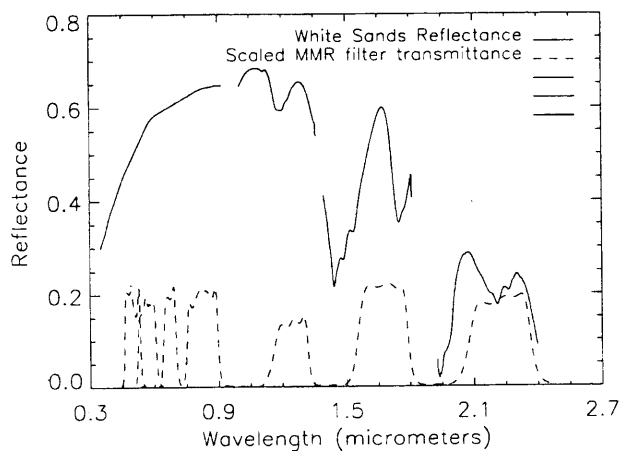


Figure 1. White Sands surface reflectance data from the ASD FieldSpec FR from September 5, 1996. Also shown in the figure are scaled MMR filter transmittances.

Radiative Transfer Code

The results from the atmospheric and surface characterizations are used in a Gauss-Seidel iteration, radiative transfer code to compute top-of-the-atmosphere radiances (Herman and Browning, 1965). The code assumes a plane-parallel, homogeneous atmosphere and divides this atmosphere into layers to account for the vertical distribution of scatterers. Weak, ozone absorption in the Chappuis band is treated within the code. The effect due to strong absorption by water vapor is treated separately by multiplying the radiative transfer code results by the water vapor transmittance for the sun-to-ground-to-sensor path. A Junge parameter derived from the solar radiometer measurements is used to compute Mie-scattering phase functions used in the code. We convert relative radiances given by the code to absolute radiances by multiplying by band-averaged solar irradiance data (Iqbal, 1983).

Irradiance-based method

The reflectance-based approach relies on numerous assumptions about the size and composition of the aerosols in the atmosphere. If these assumptions are incorrect, then the computed radiance at the top of the atmosphere is in error. In order to avoid the problems of some of these assumptions, the irradiance-based approach was developed (Biggar *et al.*, 1990b). This method uses measurements of the downwelling, global and diffuse irradiances in order to determine the radiance at the top of the atmosphere according to

$$L_{\lambda}(\theta_v, \theta_s, \Delta\phi) = \frac{E_{0\lambda} \cos(\theta_s)}{\pi} \left[\rho_{A\lambda}(\theta_v, \theta_s, \Delta\phi) + \rho_{\lambda} (1 - \rho_{\lambda} S_{\lambda}) \left(\frac{e^{-\delta_{\lambda}/\cos(\theta_v)}}{1 - \alpha_{v\lambda}} \right) \left(\frac{e^{-\delta_{\lambda}/\cos(\theta_s)}}{1 - \alpha_{s\lambda}} \right) \right] \quad (1)$$

where

- $L_{\lambda}(\theta_v, \theta_s, \Delta\phi)$ is the radiance at the top of the atmosphere for a satellite view angle of θ_v with the sun at a zenith angle of θ_s and the difference in azimuth between the sun and view direction is $\Delta\phi$
- $E_{0\lambda}$ is the solar irradiance at the top of the atmosphere for the earth-sun distance at the time the data are acquired
- $\rho_{A\lambda}$ is the apparent reflectance that would be measured for the case of a zero-reflectance surface and apparent reflectance is $\pi L_{\lambda A}(\theta_v, \theta_s, \Delta\phi)/E_{0\lambda}$ and $L_{\lambda A}$ is the intrinsic path radiance.
- ρ_{λ} is the surface reflectance
- S_{λ} is the spherical albedo of the atmosphere, that is, the ratio of the downwelling irradiance at the ground for a given set of atmospheric conditions to the reflected irradiance for the same conditions
- δ_{λ} is the vertical, spectral optical thickness
- $\alpha_{s\lambda}$ and $\alpha_{v\lambda}$ are the diffuse-to-global-irradiance ratios with the sun at zenith angles θ_s and θ_v respectively.

Of these quantities, ρ_{λ} , δ_{λ} , $\alpha_{s\lambda}$ are measured in the field at the time of satellite overpass, $E_{0\lambda}$ is determined from the literature (Iqbal, 1993), θ_s is determined from the time of overpass, and S_{λ} and $\rho_{A\lambda}$ can be found from radiative transfer calculations based on atmospheric parameters derived using the methods described in the section on the reflectance-based approach. All that is required to compute the radiance at the sensor is to determine $\alpha_{v\lambda}$. In the case where the solar zenith angle can equal the satellite zenith angle, the diffuse-to-global ratio is measured when the sun is at this zenith angle and α_v can be determined for use in Equation 1. Of course, this assumes that the atmosphere is azimuthally homogeneous and temporally invariant between the time of actual sensor overpass and the time at which the sun is at the sensor elevation.

However, it is often the case that the sensor views the test site with a near-nadir view angle and the sun does not rise high enough in the sky. For example, the latitude of our test site at White Sands Missile Range is 32.5 degrees. Thus, the highest solar elevation is 81 degrees and the diffuse-to-global ratio cannot be measured for any sensor view angle that is less than 9 degrees from nadir. In these cases, measurements throughout the morning are extrapolated to the appropriate geometry. This approach again assumes that the composition of the atmosphere does not change with time.

Diffuse-to-global measurements

The diffuse-to-global measurements used in this work were made with a recently-developed instrument (Crowther, 1997). This system is similar in philosophy to shadow-band radiometers (Harrison *et al.*, 1994) but uses a disk to block the sun rather than a shadow-band. This reduces the amount of diffuse radiance blocked while occulting the sun for the diffuse measurements. The device uses an integrating sphere to collect the downwelling irradiance. A LiCor, LI1800 spectrometer is used to measure the global and diffuse irradiance at intervals as small as 1-nm from 300 to 1100 with FWHM bandpasses of 12 nm. The advantage of this instrument over methods used in the past is that it is much less labor intensive and the measurements of the diffuse irradiance are more repeatable.

Determination of Image DNs

To determine the sensor gain (in units of DN/unit radiance), we average the DNs for the 64 pixels of interest from the image data of the White Sands region. We find these pixels in the image data by locating blue tarpaulins that were placed on the ground at the time of sensor overpass at two corners of the 64-pixel area. The tarpaulins appear bright in band 1 of TM and dark in several other bands allowing them to serve as ground control points in the imagery. In the current work, radiometrically- and geometrically-corrected image data are used based on NLAPS. This method of processing is slightly different from that used in past work that relied on Level 0 and Level 1 data from the Eosat Company. Level 0 data are unprocessed, or raw, data. Level 1 data are those that have been geometrically and radiometrically corrected. These Level 0 and Level 1 data are

somewhat comparable to the A and P formats used in the original TM Image Processing System (TIPS) used in the early days of Landsat. One key difference in the two methods is that the TIPS attempted to correct for changes in system response while the Level 1 processing relies on prelaunch calibration coefficients.

From a radiometric standpoint, it is best to use raw data for evaluating the degradation of the system since the geometric resampling that is done to produce the Level 1 and NLAPS products destroys the radiometry of the problem. However, corrected TM data have been used several times because it was often easier, and less costly, to obtain. Thome *et al.* (1994) evaluated the effect of using Level 1 instead of Level 0 data for determining the calibration coefficients for TM and found that the differences in the retrieved calibrations (<0.5%) were much smaller than the uncertainties in the reflectance-based approach (5%). This is expected because the area of White Sands that we use is relatively uniform with the change in DN from pixel to pixel being less than 1% for the first four bands of TM for the days used to evaluate the effect of relying on geometrically-corrected data. Thus, using geometrically corrected data for vicarious calibration will typically not lead to large uncertainties in retrieved calibration coefficients.

Uncertainty estimates

We give only a brief discussion of the errors in the methods used in this paper because past work discusses these errors in detail (Biggar *et al.*, 1994). There are four basic areas of uncertainty in the reflectance-based and irradiance-based approaches: atmospheric characterization, surface characterization, radiative transfer code, and computation of the site-average DNs.

The factor leading to uncertainties in determining the site's average DNs are incorrect determination of the site's location in the image leading to a misregistration between the measured site reflectance and the image DNs. As discussed in a previous section, the use of tarpaulins allows us to determine the location of our site to better than one pixel. The uncertainty due to a one pixel misregistration typically leads to less than 1% uncertainty in the site-averaged DNs and thus the computation of the calibration coefficient. This uncertainty is present in both the irradiance- and reflectance-based approaches.

The uncertainties caused by the radiative transfer code are its inherent numerical accuracy and assumptions about the vertical distribution of scatterers. Biggar *et al.* (1994) lists the uncertainty due to these as less than 1% in the top-of-the-atmosphere radiance computed by the code. In order to determine the spherical albedo and intrinsic, apparent reflectance (S_λ and $\rho_{\lambda\lambda}$ in Equation 1), the 6S code is used. While not as accurate as a full, radiative transfer code, this code is used instead of the Gauss-Seidel because these parameters are directly computed in 6S while they must be derived from the radiance field of the Gauss-Seidel. Because this work uses a bright surface with low aerosol loading there is little error caused by using the more approximate code. In addition, uncertainties in the spherical albedo and intrinsic apparent reflectance are of opposite sign and thus mostly cancel one another.

A term that is critical to both methods is the surface reflectance. We have determined that uncertainties in the

retrieval of the site's surface reflectance are less than 0.01 in surface reflectance, or alternatively, the error is less than 2% at a surface reflectance of 0.5. The primary uncertainty sources for the surface reflectance retrieval are the calibration of our field reference panels, instrumental uncertainties in our field radiometers, and diffuse-skylight corrections.

For the reflectance-based approach, our largest uncertainty source is the characterization of the atmosphere over our test site. This is mostly due to uncertainty in determining the aerosol size distribution and the aerosol complex index of refraction. These two parameters lead to top-of-the-atmosphere radiance uncertainties of 3.0% and 2.0%, respectively. This uncertainty is avoided for the most part in the irradiance-based approach since these parameters are used to determine the spherical albedo and intrinsic, apparent reflectance. As previously described, an error in one of these is mostly balanced by a similar error but of the opposite sign in the other quantity.

Uncertainties in the irradiance-based approach that are not part of the reflectance-based approach are those associated with measuring the diffuse-to-global ratio. These have been previously described for the parasol and reflectance panel approach and lead to a 2-3% uncertainty in the predicted radiance. Preliminary studies of the new instrument to measure diffuse-to-global ratios indicate this uncertainty should now be reduced to 1-2%.

All of these error sources considered together lead to total uncertainties of 5.0% for the reflectance-based approach and 3.5% for the irradiance-based approach. Of course, larger uncertainties arise when clouds or blowing sand invalidate our assumptions of horizontal homogeneity and temporal invariability. The lack of atmospheric homogeneity also affects the accuracy of surface reflectance measurements, due to differences in both the downwelling diffuse and the directly transmitted solar irradiances between the measurements of the site and those of the reflectance panel. These problems are minimized by selecting dates for which the measured aerosol optical depths do not vary significantly with time. This has been done for the calibration described in this paper. In addition, the uncertainty values presented here are strictly valid for a typical White Sands case in the visible and near-infrared, bands 1-4 for TM. Results in the shortwave infrared, bands 5 and 7, are slightly more degraded because of greater uncertainty in the site's surface reflectance due to greater reference-panel-calibration uncertainty and lower site reflectance.

RESULTS

The above-described approaches were applied to data collected on December 16, 1996 to determine a calibration for Landsat-5 TM. The Landsat overpass was at 17:01:40 UTC at a sensor view of 0.2 degrees from nadir. The solar zenith angle at this time was 63.1 degrees and the difference in azimuth between the satellite's line of sight and the sun was 45.1 degrees. **Figure 2** shows the measured, non-molecular, scattering optical depth as a function of time for 440 and 870 nm for the entire period for which data were collected on this date. It can be seen from the figure that the day was clear and there was very little change in atmospheric turbidity during the period. The optical depths for the solar

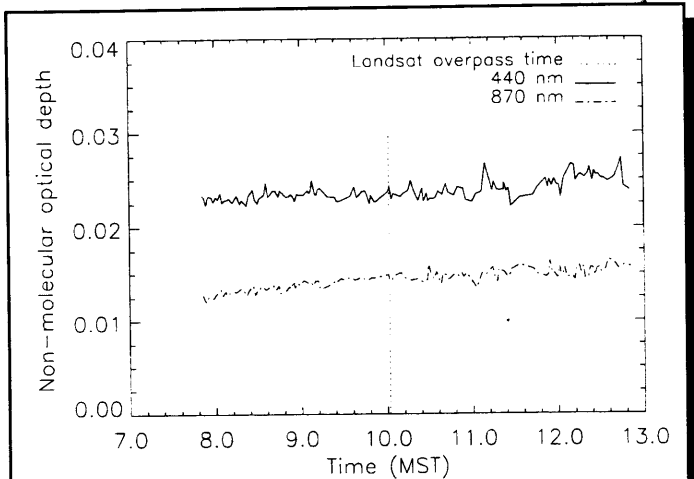


Figure 2. Non-molecular optical depths measured at White Sands on December 16, 1996 for 440 and 870 nm as a function of time. The overpass time of the Landsat-5 platform is indicated by the vertical dotted line.

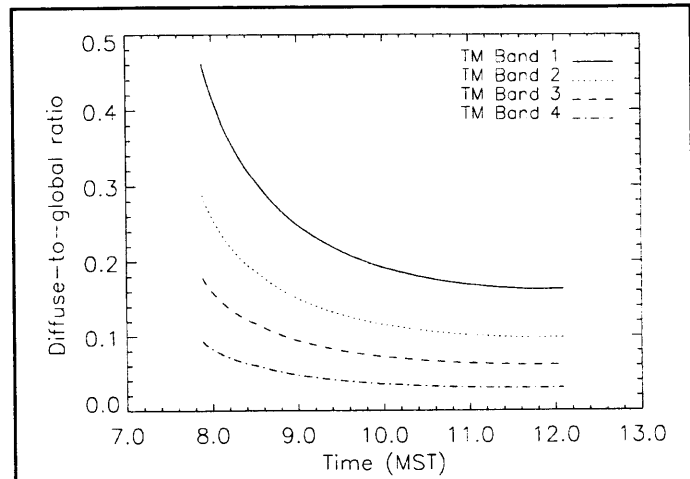


Figure 3. Diffuse-to-global ratio as a function of time for December 16, 1996 at White Sands for the four TM bands in the visible and near infrared part of the spectrum.

radiometer bands not affected by water vapor absorption were averaged for the ten-minute period about the time of the sensor overpass. These average optical depths were inverted to give a Junge parameter of 2.54 and a columnar ozone amount of 0.22 cm-atm. This Junge parameter and columnar ozone were used to determine the optical depths for the center wavelengths of the six, solar-reflective bands of TM. The columnar water vapor was found to be 0.45 cm and this was used to determine the gaseous transmittance for the sun-to-ground-to-sensor path using 6S.

The surface reflectance in each band was determined from band-averaging the spectral surface reflectance determined from the 640 points from the ASD FR measurements of the TM site. These results are shown in **Table 2**. The standard deviation of the average of the ASD FR results based on the center wavelength of each TM band are shown for reference. The band-centered value is here for simplicity and this standard deviation is a slowly varying function of wavelength. The spectral shape of these data are very similar to that shown in **Figure 1**.

Figure 3 shows the measured, diffuse-to-global ratio for the center wavelength of the first four bands for TM for the same

period as shown in **Figure 2**. This figure confirms that the atmospheric variations due to sharp changes in aerosol loading or clouds did not occur during the measurement period since the curves shown in the figure are smooth. The shape of these curves can be understood by first realizing the cosine dependence of the global irradiance due to the change in sun angle with time. At low solar elevation angles early in the day, the solar energy incident on the spherical collector is low because of the longer path at this time of the day. In addition, the angle of incidence between the collector and the solar beam is large leading to a low irradiance from the incident-angle cosine. At these solar angles, scattering by the atmosphere dominates, thus, the ratio of the diffuse irradiance to the global irradiance should be larger than later in the morning when the sun is higher in the sky. The amount of diffuse irradiance is larger later in the morning than when the sun is lower in the sky due to lower attenuation of the solar beam. However, the amount of directly transmitted solar energy is much larger than early in the morning and this effect dominates. Thus the ratio of diffuse to global irradiances decreases with time as shown in the figure. If a full-day's data set were collected, then the curve would increase after solar

Table 2.

December 12, 1996 surface reflectance results from White Sands using band-averaged ASD FR results. Also shown are the 1σ standard deviations of the average of the ASD FR results and the inputs needed to compute the at-sensor radiance for the irradiance-based method.

TM band	Reflectance	1- σ std. dev.	$E_{0\lambda}$ (W/m ² /μm)	$\alpha_{S\lambda}$	$\alpha_{V\lambda}$	$\rho_{A\lambda}$	S_{λ}	δ_{λ}
1	0.476	5.4%	2019	0.191	0.114	0.070	0.114	0.166
2	0.560	5.5%	1887	0.115	0.066	0.036	0.068	0.119
3	0.594	5.6%	1596	0.072	0.042	0.021	0.042	0.069
4	0.637	5.5%	1077	0.036	0.019	0.009	0.019	0.030
5	0.583	6.8%	227.4	-	-	-	-	-
7	0.178	14.6%	76.92	-	-	-	-	-

noon as the sun moves towards sunset. The values for band 1 of TM are larger because the larger amount of molecular and aerosol scattering leads to a higher scattering optical thickness than at other wavelengths. This increased scattering leads to a larger diffuse component and lower direct solar irradiance, and hence, a larger ratio. **Table 2** shows the measured values for $\alpha_{v\lambda}$ for each of the four bands at the time of sensor overpass. Also shown are the extrapolated values for $\alpha_{v\lambda}$ as well as values for the spherical albedo and intrinsic, apparent reflectance found using 6S, and the optical thicknesses.

Table 3 shows the results from the irradiance- and reflectance-based methods. Since the LI1800 only collects data out to 1100 nm, results for the irradiance-based approach are only shown for the first four bands. The differences seen in the table are on the order of 1-6%. These values are within the combined uncertainties of the methods (5% for the reflectance-based and 3.5% for the irradiance-based method). However, in all four bands, the irradiance-based results are lower than the reflectance-based. It is also interesting that the smallest difference occurs for band 4 which has the lowest aerosol and molecular scattering optical depths of the bands used. Some of this difference is due to the uncertainties in the inputs between the two methods, but it is difficult to determine the specific causes due to the complex interactions between the various inputs. Changing the value of a single parameter (such as optical thickness, aerosol size distribution, aerosol refractive index) is not sufficient to bring the results of the two methods into significantly better agreement. Further study is required to determine whether there is a bias between the two approaches.

In addition to comparing the results from the two vicarious calibration techniques, it is also possible to look at the radiances that are obtained by converting the average DNs for the test site to radiance using calibration gains and biases supplied with the image data. The average DNs were determined using the method described above and are given in **Table 3**. The standard deviation of the average of the 64 pixels ranged from 1.2% for band 4 to 3.4% for band 7. The uncertainty caused by a one-pixel misregistration ranged from 0.1% in band 1 to 0.8% in band 5. These DNs were converted to radiance using

$$L_{\lambda} = G_{\lambda} \times DN_{\lambda} + B_{\lambda}$$

where G_{λ} and B_{λ} are the gain and bias reported on the tape for a given band and are given in **Table 3**. From the table it is clear that there is better agreement between the irradiance-based method and the tape values than for the reflectance-based approach. However, if band 5 is ignored, the differences between all three methods are <19% for band 2 and <13% or less for other bands.

For completeness we include results from previous work at White Sands using the reflectance-based approach. These results are shown in **Table 4**. The missing portions of the table for band 1 correspond to dates where saturated image data were reported for the site. The missing portions of bands 5 and 7 are due to missing surface reflectance data in these bands. These results have been previously reported and described elsewhere (Thome *et al.*, 1993, Thome *et al.*, 1994). The most important thing to note is the large discrepancy between these results and the current ones from the NLAPS data set. The explanation for this is that the DNs in the NLAPS data set have been scaled in a different fashion than the data used to obtain the results in **Table 4**. This points out the critical need for users of Landsat data to ensure that the appropriate calibration is used to convert from image DN to radiance. Plans are currently underway to attempt to compute calibration coefficients for the dates shown in **Table 4** using DNs determined from the NLAPS data sets.

CONCLUSIONS

The reflectance- and irradiance-based methods have been used to perform a vicarious calibration of Landsat-5 TM. This is the first application of the irradiance-based approach to Landsat TM and is of interest because past work has not included a band in the blue portion of the spectrum. The radiances predicted at the top of the atmosphere using these two methods agree with each other to better than 6% with better agreement at the longer wavelength bands. The results agree within the estimated uncertainties of the methods, but the irradiance-based results give radiances that are all lower than the reflectance-based

Table 3.

Comparison of radiances predicted by the reflectance- and irradiance-based approaches. Radiances determined by applying the NLAPS gains and biases to the image data digital numbers (from the 64-pixel average) are also given for comparison and are listed as the image-based radiances.

TM band	Radiances ($W/m^2/sr/\mu m$)			Average site digital numbers	NLAPS gain ($Watts/m^2/sr/\mu m/DN$)	NLAPS bias ($Watts/m^2/sr/\mu m$)
	Reflectance	Irradiance-based	Image-based			
1	136.6	128.0	121.0	203.3	0.602	-1.520
2	137.1	130.9	115.2	100.5	1.175	-2.840
3	127.5	124.4	112.5	141.0	0.806	-1.170
4	94.95	94.12	87.96	109.8	0.814	-1.510
5	17.76	-	12.23	116.6	0.108	-0.370
7	1.782	-	1.795	34.1	0.057	-0.150

Table 4.

Radiances ($\text{Wm}^{-2}\text{sr}^{-1}\mu\text{m}^{-1}$) per unit DN for the dates shown and for the six solar reflective bands of Landsat-5 TM based on level-0 data (or equivalent).

Date	Band 1	Band 2	Band 3	Band 4	Band 5	Band 7
Preflight	0.643	1.272	0.980	0.924	0.127	0.068
1984-07-8		1.362	1.047	0.948		
1984-10-28	0.720	1.366	1.079	0.920	0.142	0.067
1985-05-24		1.335	1.062	0.957		
1985-08-28		1.399	1.094	0.892	0.138	0.066
1985-11-16	0.732	1.397	1.085	0.914	0.133	0.062
1987-03-27	0.765	1.425	1.122	0.954	0.134	0.062
1988-02-10	0.767	1.387	1.089	0.944	0.136	0.061
1992-08-15		1.536	1.133	0.954	0.135	0.065
1993-10-21	0.781	1.464	1.082	0.914	0.134	0.066
1994-10-8	0.818	1.531	1.127	0.949	0.147	0.076

approach. Also, the largest difference is for band 1, the band most affected by atmospheric effects. Thus, future work will concentrate on seeing if there is a bias between the results. These comparisons should be much easier to obtain through the use of the newly-developed diffuse-to-global instrument that was used for this work.

The vicarious results are also compared to radiances determined from gains and biases determined from NLAPS. The agreement with the NLAPS results are better for the irradiance-based results, but agreement between all three results approaches, or is within the combined uncertainties of the methods used to retrieve the radiances in most bands. This is encouraging for two reasons. First, it shows that users may be able to use calibration coefficients supplied with the data for some applications where the estimated 10% calibration of TM is sufficient. This is not true of other TM processing schemes which only supply preflight calibration data with the imagery. The agreement also indicates the usefulness of the irradiance-based method, though further work is needed to better understand the discrepancies between the reflectance-based and irradiance-based approaches especially at shorter wavelengths such as TM band 1.

The results are also compared to historical results since 1984. The difference between the gains computed from the historical data and the NLAPS show large discrepancies that are due to differences in the processing of the image data. These discrepancies point to two conclusions. The first is that users must take care to ensure that the appropriate gains are used for their given data set. The second conclusion is that these discrepancies make a case for consistent processing of data sets. Plans are currently underway to determine the gains for the dates shown in Table 4 using NLAPS data so that a history of the calibration coefficients similar to that shown in the table can be developed.

ACKNOWLEDGEMENTS

The authors wish to acknowledge the Atmospheric Sciences Laboratory at White Sands Missile Range for on-site support for our field campaigns and Rob Kingston for assistance in reading the image tapes, and Wayne Boncyk at the Eros Data Center for his assistance in understanding the NLAPS data format. We would like to express thanks to the Landsat-7 Project Science Office, and especially to Tom Brakke, at Goddard Space Flight for assistance in obtaining the Landsat-5 data. This work was performed with support from NASA contract NAS5-31717 and NASA Grant NAG-53436.

REFERENCES

- Balick, L. K., C. J. Golanics, J. E. Shines, S. F. Biggar, and P. N. Slater. 1991. "The in-flight calibration of a helicopter-mounted Daedalus multispectral scanner," *Proc. Spie*, Vol. 1493, pp 215-223.
- Biggar S. F., D. I. Gellman, and P. N. Slater. 1990a. "Improved evaluation of optical depth components from Langley plot data," *Rem. Sens. Env.*, Vol. 32, pp. 91-101.
- Biggar, S. F., J. Labeled, R. P. Santer, P. N. Slater, R. D. Jackson, and M. S. Moran. 1988. "Laboratory calibration of field reflectance panels," *Proceedings of SPIE*, Vol. 924, pp. 232-240.
- Biggar, S. F., M. C. Dinguirard, D. I. Gellman, P. Henry, R. D. Jackson, M. S. Moran, and P. N. Slater. 1991. "Radiometric calibration for SPOT-2 HRV - a comparison of three methods," *Proc. Spie*, Vol. 1493, pp. 155-162.
- Biggar, S. F., R. P. Santer, and P. N. Slater. 1990b. "Irradiance-based calibration of imaging sensors," *International Geoscience and Remote Sensing Symposium*, College Park, Maryland, pp. 507-510.
- Biggar, S. F., P. N. Slater, and D. I. Gellman. 1994. "Uncertainties in the in-flight calibration of sensors with reference to measured ground sites in the 0.4 to 1.1 μm range," *Rem. Sens. Env.*, Vol. 48, pp. 242-252.
- Crowther, B. G. 1997. *The design, construction, and calibration of a spectral diffuse/global irradiance meter*. Ph. D. dissertation, University of Arizona, 140 pp.
- Gellman, D. I., S. F. Biggar, M. C. Dinguirard, P. J. Henry, M. S. Moran, K. J. Thome, and P. N. Slater. 1993. "Review of SPOT-1 and -2 calibrations at White Sands from launch to the present," *Proc. SPIE*, Vol. 1938.
- Gellman, D. I., S. F. Biggar, P. N. Slater, and C. J. Bruegge. 1991. "Calibrated intercepts for solar radiometers used in remote sensor calibration," *Proc. SPIE*, Vol. 1493, pp. 19-24.
- Harrison, L., J. Michalsky, and J. Berndt. 1994. "Automated multifilter rotation shadow-band radiometer: an instrument for optical depth and radiation measurements," *Appl. Opt.*, Vol. 33, pp. 5118-5125.
- Herman, B. M. and S. R. Browning. 1965. "A numerical solution to the equation of radiative transfer," *J. Atmos. Sci.*, Vol. 22, pp. 559-566.
- Iqbal, M. 1983. *An Introduction to Solar Radiation*, Academic Press, New York, pp. 379-381.

Robinson, B. F., M. E. Bauer, D. P. Dewitt, L. F. Silva, and V. C. Vanderbilt. 1979. "Multiband radiometer for field research," *Proc. SPIE*, Vol. 196, pp. 8-15.

Slater, P. N., S. F. Biggar, R. G. Holm, R. D. Jackson, Y. Mao, M. S. Moran, J. M. Palmer, and B. Yuan. 1987. "Reflectance- and radiance-based methods for the in-flight absolute calibration of multispectral sensors," *Rem. Sens. Env.*, Vol. 22, pp. 11-37.

Thome, K. J., B. M. Herman, and J. A. Reagan. 1992. "Determination of precipitable water from solar transmission," *J. Appl. Meteor.*, Vol. 31, pp. 157-165.

Thome, K. J., C. L. Gustafson-Bold, P. N. Slater, and W. H. Farrand. 1996. "In-flight radiometric calibration of HYDICE using a reflectance-based approach," *Proc. SPIE Conf.* 2821, Denver, Colorado.

Thome, K. J., D. I. Gellman, R. J. Parada, S. F. Biggar, P. N. Slater, and M. S. Moran. 1993. "In-flight radiometric calibration of Landsat-5 Thematic Mapper from 1984 to present," *Proc. SPIE Conf. #1938*, Orlando, Florida, pp. 126-131.

Thome, K. J., S. F. Biggar, D. I. Gellman, and P. N. Slater. 1994. "Absolute-radiometric calibration of Landsat-5 Thematic Mapper and the proposed calibration of the Advance Spaceborne Thermal Emission and Reflection Radiometer," *International Geoscience and Remote Sensing Symposium*, Pasadena, pp. 2295-2297.

Best Western International Corporate Rate Program

Best Western International is pleased to welcome members of the Canadian Aeronautics and Space Institute to our Corporate Rate Program. Our program is designed to meet all of the needs for your business travel worldwide.

To receive your discount of 10-15% off regular rates at any one of our 3,800 properties worldwide just use our toll free reservations line at 1-800-528-1234 and quote your Best Western International Corporate Number #01268770.

For information on meeting, conference or seminar requirements please call toll free 1-888-608-1888 and ask for our Meetings Resource Guide and Ontario/Quebec Business Directory.

